# Islanding Detection of Inverter Interface Distributed Generator in Microgrid

[1] Vishakha Rajkumar Kelwatkar, [2]Prof. Nilima B. Dhande

[1]Reseach Scholar, [2]Assistant Professor
[1,2] Electrical Engineering Department,
[1,2] Shri. Sai College of Engineering and Technology, Bhadrawati, Maharashtra, India

*Abstract :* The term "distributed generation" refers to a new type of energy source that is employed in distribution networks. Customers or distribution system operators link DGs directly or indirectly. DGs are often linked near consumer load centres. The increased usage of DGs results in improved power quality, a better voltage profile, and a reduction in losses.
Because dispersed energy resources are becoming more important in power systems, their issues should be investigated. Unplanned islanding is one of the most serious issues with dispersed energy supplies. The power systems and the repairmen who are working with the wrong equipment are both at risk as a result of the unexpected islanding. The suggested technique uses the wavelet transform as well as a novel classifier called Back-propagation Artificial Neural Network (BP-ANN) and Adaptive Neuro Fuzzy Inference System (ANFIS). To extract characteristics from the current waveform at the point of common coupling (PCC), the wavelet transform is utilised. PCC is believed to be the distribution system's connecting point for dispersed generating. In MATLAB/SIMULINK software, the suggested technique is implemented on a two PV array 40 KW as a Distributed generating system. The findings demonstrate the suggested method's excellent accuracy in detecting islanding.
At last, comparison of ANFIS and BP-ANN approach is done and finally conclusion provide for best classifier for islanding detection for distributed generator system.

***Index Terms* – Islanding detection, Distributed generators, Solar PV array system**

## I. INTRODUCTION

DG penetration in distribution networks has a negative impact on protection coordination. Over-current (OC) relays, differential current relays, circuit breakers, re-closers, and fuses are all examples of conventional distribution protection devices.
The traditional OC protection is designed for radial distribution systems with a fault current that tends to flow in one direction. The integration of distributed energy resources (DERs) into the distribution system, on the other hand, transforms single-fed radial systems into complicated ones that take into account several power sources. As a result, the fault current's tendency changes from unidirectional to bidirectional [4].
Protection coordination among relays, re-closers, and fuses is widely known in radial systems, however once DGs are incorporated into the systems, coordination among protective instruments is either reformed or completely lost [5]. The capacity, kind, and placement of the DGs have an impact on the degree of protective coordination [6–8]. Furthermore, false/nuisance tripping of relays, rise/fall in fault level with connection/disconnection of DERs influencing reach of OC relay, undesired islanding, prohibition of automated reclosing, and out-of-synchronism are all detrimental effects of DG penetration into the distribution system [3,9,10]. Anti-islanding protection schemes, events/fault protection schemes in grid linked mode, and events/fault protection schemes in islanded mode are the three types of micro-grid protection schemes.
When a distribution system gets electrically separated from the rest of the power system, but is still powered by DG connected to it, this is known as islanding. Traditionally, a distribution system does not have any active power producing sources and does not receive electricity in the event of a failure in the transmission line upstream, but this is no longer the case with DG. In the event of islanding, nearly all utilities now demand DG to be removed from the grid as quickly as feasible. The IEEE 929-1988 standard specifies that after DG is landed, it must be disconnected. Islanding can be done on purpose or by accident. During utility grid repair, the electrical grid may be shut down, resulting in generator islanding. The islanding is known because the loss of the grid is voluntary. The non-intentional islanding produced by an unintentional grid shutdown is of more importance. Unintentional islanding has a number of drawbacks.
Although islanding operations have certain advantages, they also have significant disadvantages. The following are a few of them: After main sources have been opened and tagged out, DG sources feeding a system might endanger line workers' safety. It's possible that the voltage and frequency won't stay within a safe range. The DG interconnection may not be sufficiently grounding the islanded system. The deterioration of electric components as a result of voltage and frequency drifts is one of the dangers that might arise as a result of this. Because of these factors, detecting islanding promptly and correctly is critical.

## II. PROPOSED METHOD

Figure 5 shows the proposed system flow block diagram in which islanding event detection of 40 KW solar PV array system as distributed generators. Solar pv system 40 kw design in matlab simulation model using base paper model specifications. PV solar array system output DC voltage is converting into three phase AC supply using three phase 180 degree mode of inverter. Solar PV array system is connected with AC grid at which load side three phase voltage and current measured and send to wavelet multi-resolution analysis for signal analysis. Wavelet spectral energy calibrated in this wavelet transform block. Calibrated energy of three phase voltages and current is measured for different islanding condition on two solar pv array system. That spectral energy is measured is act as training data set for BP-ANN and ANFIS controller for islanding generator number detection.

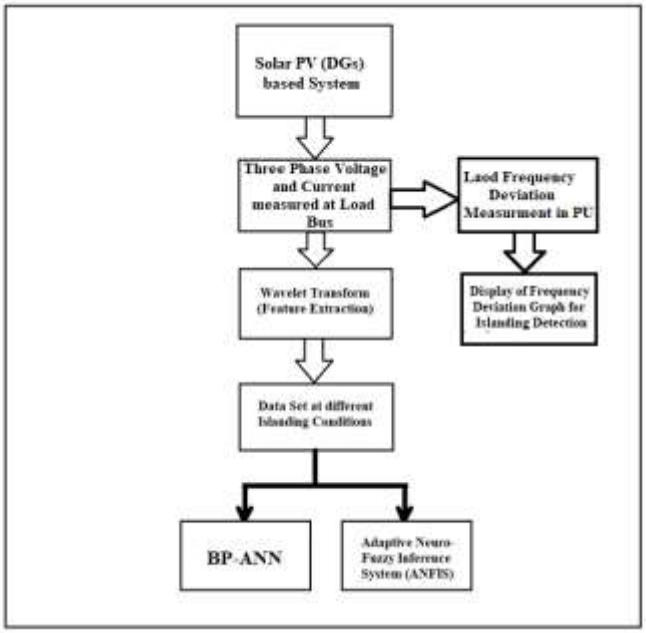


**Fig.5.** Flow block diagram of proposed islanding detection techniques

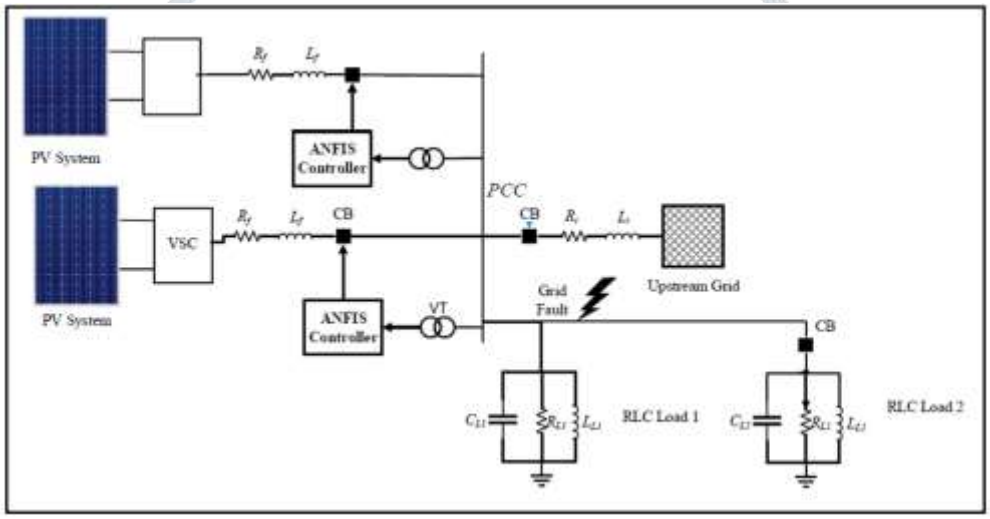


**Fig.6.** Single line diagram of two Distributed Generator Based System

The test setup for researching islanding circumstances is shown in Figure 6. The system includes a photovoltaic (PV) unit as a DER that is connected to a voltage-sourced converter (VSC), an RL filter that connects the VSC to the PCC of a 0.4 kV LV network that feeds an RLC load, and a voltage-sourced converter (VSC) that connects the VSC to the PCC of a 0.4 kV LV network that feeds an RLC load. At the VSC input, the PV is represented as a continuous current source that delivers 300 V DC voltages. With a solar irradiance of 1000 kW/m2 and a panel temperature of 25 degrees Celsius, the PV unit is set to its maximum power point.

A 20 kW PV unit is termed DG in this case. It may, however, be readily substituted with any other RERs or ESSs. Pulse width modulation (PWM) is used to create the firing signals of integrated gate bipolar transistor (IGBT) switches in the VSC. The PCC connects the DG to the DN, allowing it to function in either islanded or grid-connected mode. For the DN power source, the RLC impedance is internal. When islanding is detected, the line breaker switch is utilised to divide DG from DN. A second CB is utilised to perform further RLC load testing. According to Fig. 6, the load's power consumption is equal to the sum of the power provided to the grid and generated by the DG source, which is calculated as follows:

$$P_{load} + jQ_{load} = (P_{pv} + jQ_{pv}) + (\Delta P + j\Delta Q)$$

$P_{PV}$ and $jQ_{PV}$ are generated energy from PV system as a result of DC/AC inverter, while P and jQ are active and reactive energy provided by DN in synchronized mode of ΔP and jΔQ.

## III. SIMULATION MODEL

### 3.1 Simulation Model

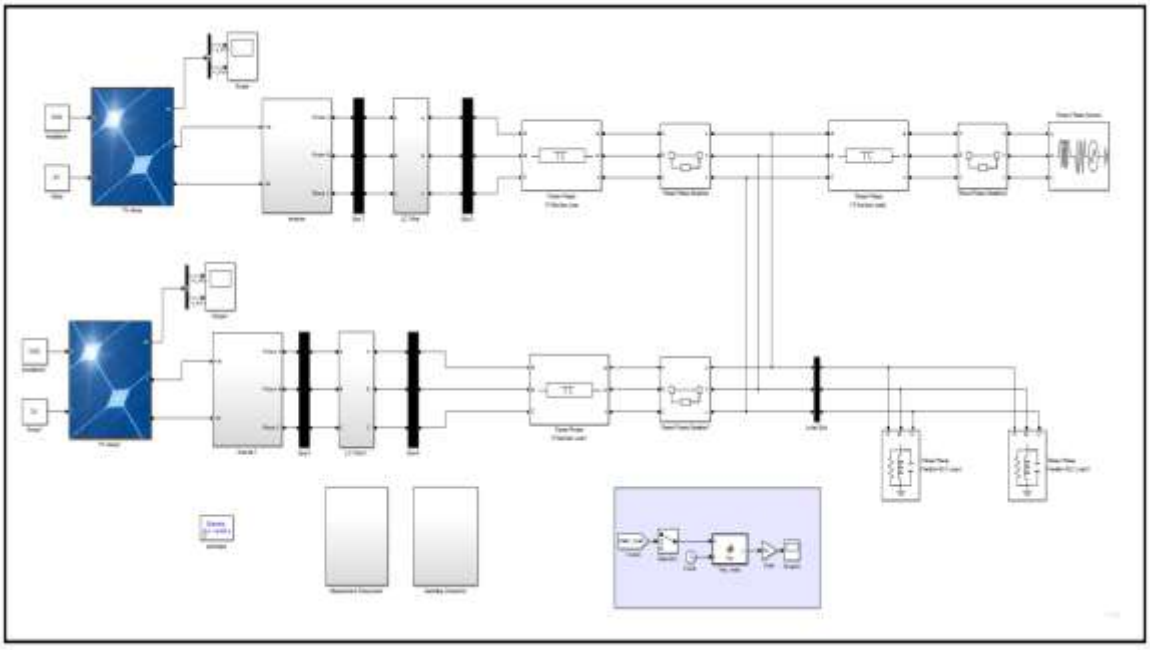

**Fig.7.** MATLAB Simulink model of two DGs sources (PV System) based power system

**Table.1.** Simulation Model of DC PV system Parameters specification

| | |
|---|---|
| Model type | Soltech 1STH-215-P |
| Maximum power | 213.15 W |
| Voltage at MPP | 29 V |
| Current at MPP | 7.35 A |
| Short circuit current | 7.84 A |
| Open circuit voltage | 36.3 V |
| Maximum system voltage | 360V |
| Series connected modules per string | 11 |
| Parallel connected strings | 11 |

**Table.2.** Power system model parameters

| | |
|---|---|
| DG Power | 21 KW |
| Inverter input DC Voltage | 300-310 V |
| PCC Voltage (L-L) | 390-400 V |
| Nominal frequency | 50 Hz |
| DN Resistance | 0.89 Ohm |
| DN Inductance | 0.016 H |
| DG Current filter inductance | 0.01 H |
| DG voltage filter capacitance | 12 KF |

Figure 7 shows the matlab simulation model of complete system. System is consist of different subsystem like Solar PV 40 KW Subsystem, three phase 180 degree mode inverter, frequency deviation subsystem, power system and three phase parallel RLC load. The specification of 40 KW solar pv system is shown in table 1 and power system specifications shown in table 2.

### 3.2 Three phase inverter and LC filter

Figure 8 shows the parallel LC filter which connected after three phase inverter output. This parallel LC filter is use for remove the $3^{rd}$ order and $5^{th}$ order harmonics content to make generated square as pure sinusoidal waveform.

Figure 10 shows the measurement subsystem in which individual bus bar i.e. Bus 1, 2, 3, 4, Load bus bar measurement like three phase rms voltage and three phase current.

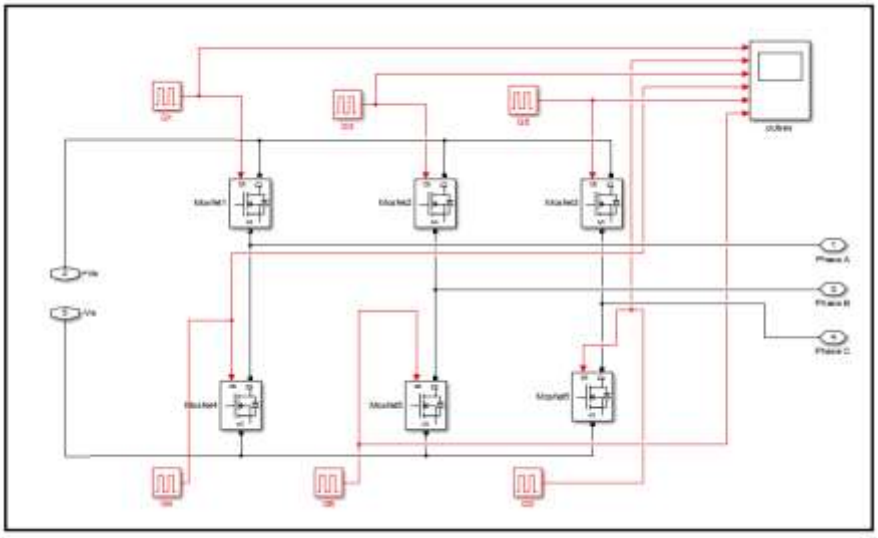

**Fig.8.** MATLAB simulation model of three phase inverter subsystem

**Table.3.** Simulation Model Parameters specification

| Sr No | Name of simulation block | Specification |
|---|---|---|
| 1. | Mosfet | FET resistance (Ron) = 0.1 Ohm<br>Internal Diode inductance Lon (H) = 0 H<br>Internal Diode resistance Rd = 0.01 Ohm<br>Snubber Resistance Rs = 100000 Ohm |
| 2. | Pulse generator (Mosfet-1) | Amplitude = 1; Period = 0.02 Sec ; Pulse width = 50 %; Phase Delay = 0 Sec |
| 3. | Pulse generator (Mosfet-2) | Amplitude = 1; Period = 0.02 Sec ; Pulse width = 50 %; Phase Delay = (60/360)*0.02 Sec |
| 4. | Pulse generator (Mosfet-3) | Amplitude = 1; Period = 0.02 Sec ; Pulse width = 50 %; Phase Delay = (120/360)*0.02 Sec |
| 5. | Pulse generator (Mosfet-4) | Amplitude = 1; Period = 0.02 Sec ; Pulse width = 50 %; Phase Delay = (180/360)*0.02 Sec |
| 6. | Pulse generator (Mosfet-5) | Amplitude = 1; Period = 0.02 Sec ; Pulse width = 50 %; Phase Delay = (240/360)*0.02 Sec |
| 7. | Pulse generator (Mosfet-6) | Amplitude = 1; Period = 0.02 Sec ; Pulse width = 50 %; Phase Delay = (300/360)*0.02 Sec |

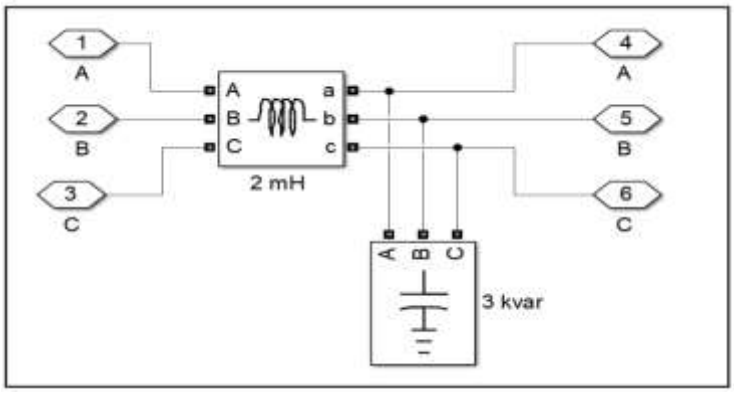


**Fig.9.** LC Filter subsystem model design in matlab simulation

### 3.3 Wavelet transform subsystem

**Table.4.** Wavelet multi-resolution analysis subsystem specification

| Sr No. | Parameters | Specification |
|---|---|---|
| 1. | Number of multi-resolution analysis levels | 04 |
| 2. | Name of mother wavelet | Daubechies |
| 3. | Type of mother wavelet | Db3 |

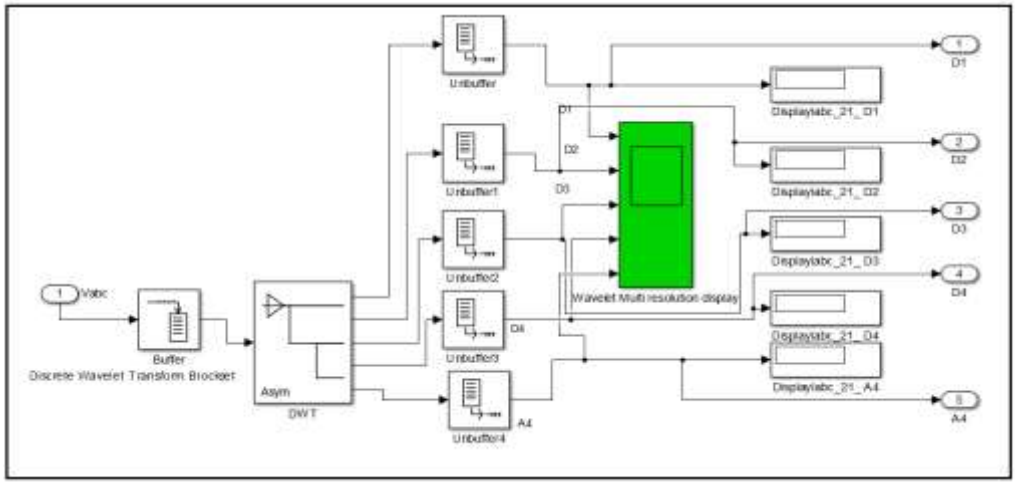


**Fig.11.** Matlab simulation of wavelet multi-resolution subsystem model

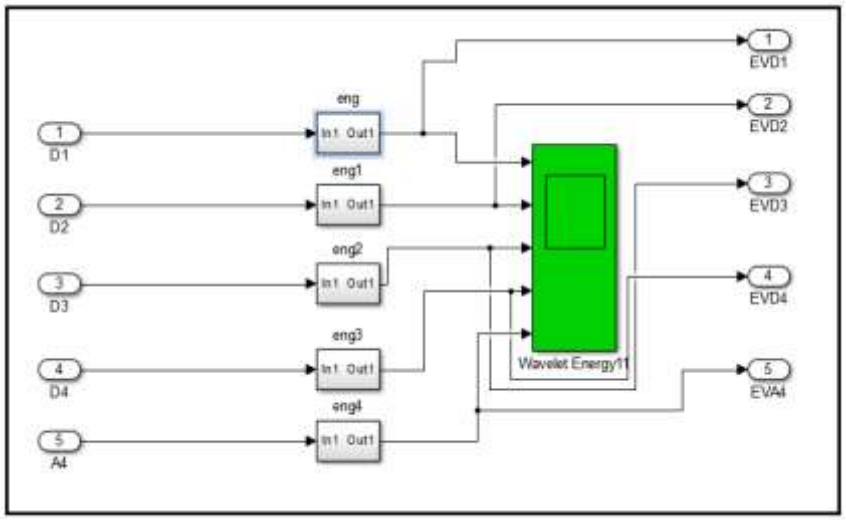


**Fig.12.** Energy calibration subsystem at each output of wavelet transform

Figure 11 shows the wavelet multi resolution analysis subsystem with spectral energy calibration subsystem shown in figure 12. The total four level use for multi-resolution analysis using Daubechies 2 (Db2) mother wavelet. Input for mother wavelet is input three phase current measured at bus bar 7 of IEEE system while output is wavelet features of Detail D1 to D4 and Approximation A4 at level 4. Then after spectral energy of D1 to D4 and A4 are calibrated using spectral energy calibration subsystem connected at each signal shown in figure 13.

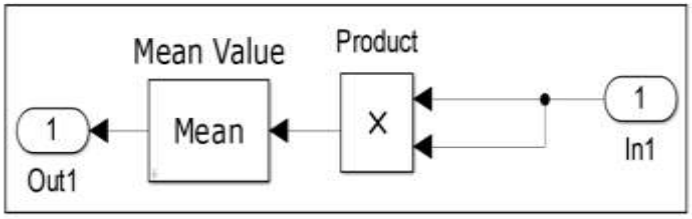


**Fig.13.** Energy calibration formula implementation in matlab simulation

Figure 14 shows ANFIS and ANN subsystem in matlab simulation model. In this case, three phase rms voltage and current is send to wavelet multi-resolution analysis. Then after multi-resolution analysis spectral energy of detail and approximate signal calculated. Spectral energy of three phase voltages is send to ANFIS controller for detection of islanding DG generator number. Also, Three phase voltage and current wavelet spectral energy 10 inputs of details and approximate signals are send to BP-ANN for classification of islanding generator number detection.

Figure 16 shows the frequency deviation method for islanding event detection of connected distributed generator system. During islanding condition, there is frequency variation occurs in power system for short duration of time. That frequency deviation is make the power system component saturation. Hence, that saturation level may be cause damage of power system components like transformer, loads etc.

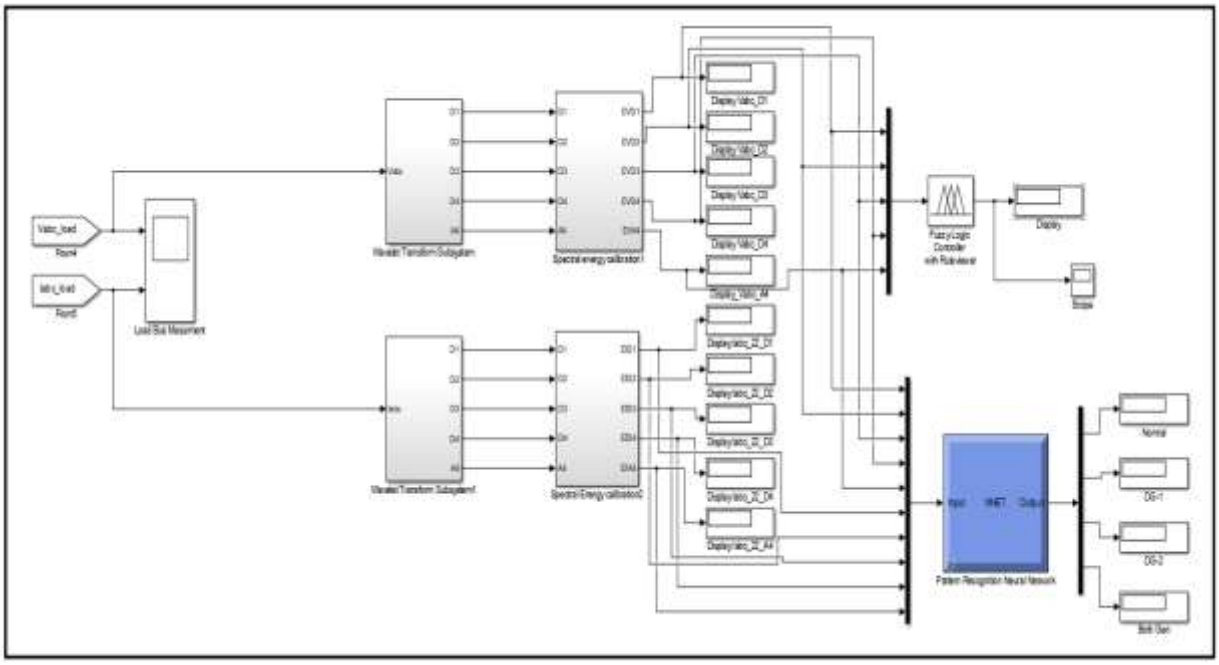

**Fig.14.** Matlab simulation model of wavelet transform, ANN and ANFIS subsystem for islanding detection

### 3.4 Frequency deviation detection subsystem

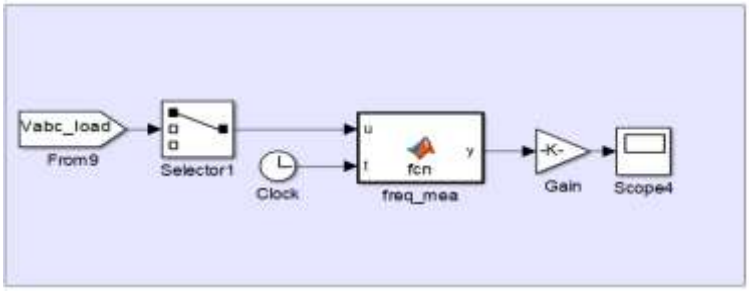


**Fig.15.** Matlab model of Frequency deviation measurement subsystem during islanding condition

```
function y = fcn(u,t)
%#eml
  persistent  uk tk
g
  if isempty(uk)
      uk=0;
      tk=0;
      y=50;
      g=0;
      return
  end
  if u>0 && uk<0
      g=t-tk;
      tk=t;
  end

  if tk ~= 0
      y=1/g;
      if y>50.2
          y=50.1;
      end
  else
      y=50;
  end
%   if t<0.25
%       y=50;
%   end

  uk=u;
```

**Fig.16.** Matlab function for frequency deviation detection

## IV. SIMULATION RESULTS

### 4.1 Normal Condition

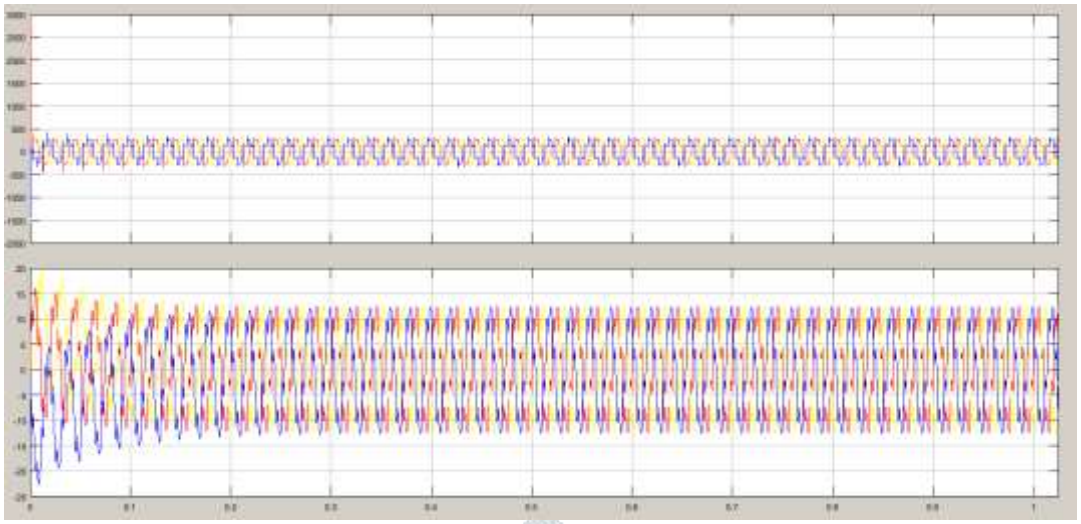

**Fig.17.** Three phase voltage and current measured at inverter output at bus bar 1 during normal condition

Figure 17 shows three phase voltage and current measured at bus bar 1 i.e. AC output of solar PV array system-1 (40KW) during normal condition. Upper Y axis represent the three phase voltage in volts and lower Y axis shows the three phase current in Ampere. During normal condition, the three phase voltage and current becomes normal and rated.

Figure 18 shows three phase voltage and current measured at bus bar 2 i.e. AC output of solar PV array system-2 (40KW) during normal condition. Upper Y axis represent the three phase voltage in volts and lower Y axis shows the three phase current in Ampere. During normal condition, the three phase voltage and current becomes normal and rated.

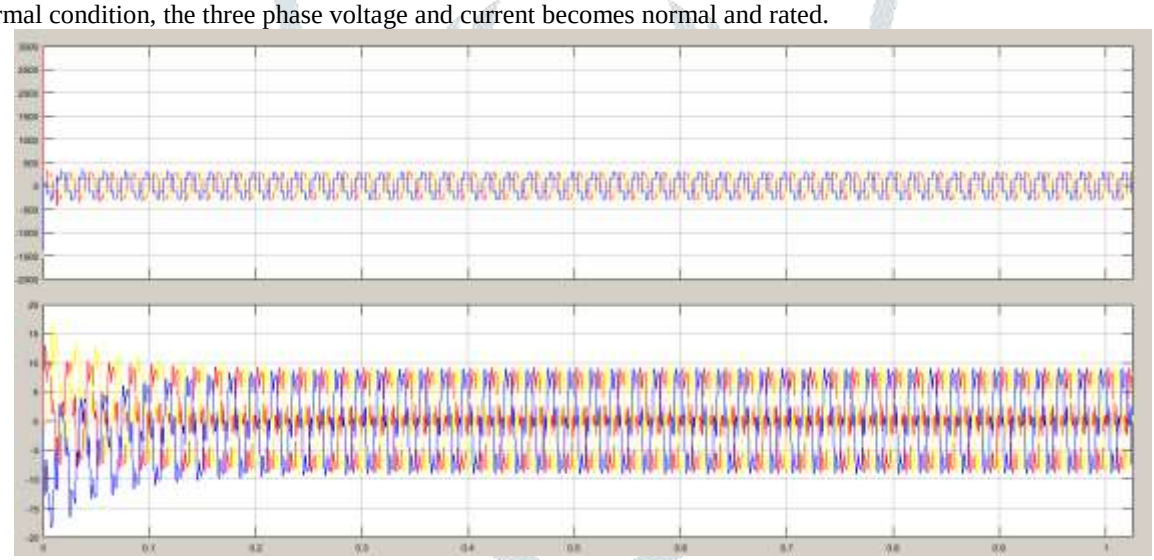

**Fig.18.** Three phase voltage and current measured at inverter output at bus bar 2 during normal condition

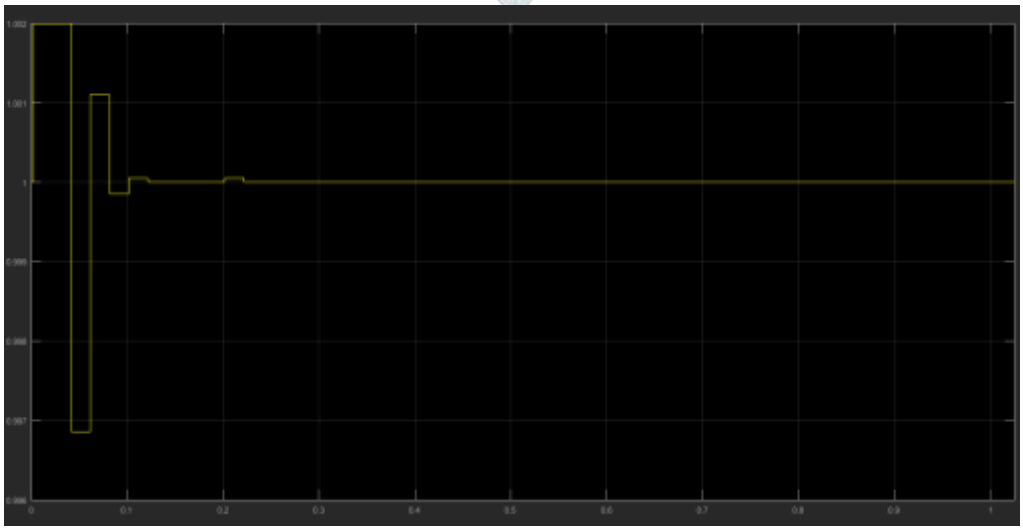

**Fig.19.** Frequency deviation measurement during normal condition at load bus bar

Figure 19 shows the frequency verses simulation time. In which here on Y axis is show frequency in Hz and X axis shows the simulation time in second. During initial time upto 0.1 sec time, there is variation in frequency due transient state of power system

(initial settling time period). Then after 0.1 Sec there is no any frequency deviation. Throughout the operation frequency becomes 50 Hz constant.

### 4.2 Case-2 Islanding at DG- 1

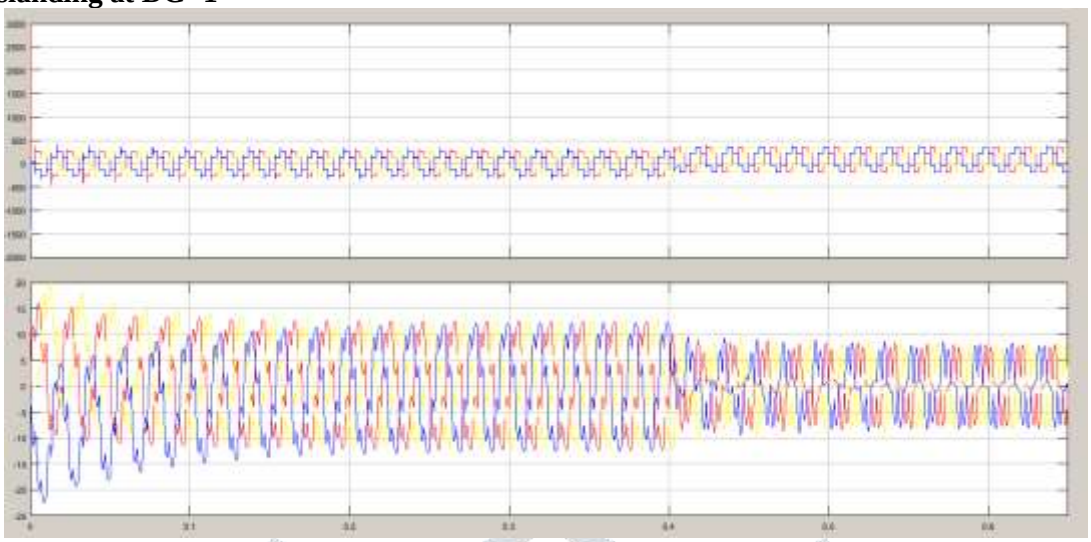

**Fig.20.** Three phase voltage and current measured at bus bar 1 during islanding occurs at 0.4 sec on DG-1 system

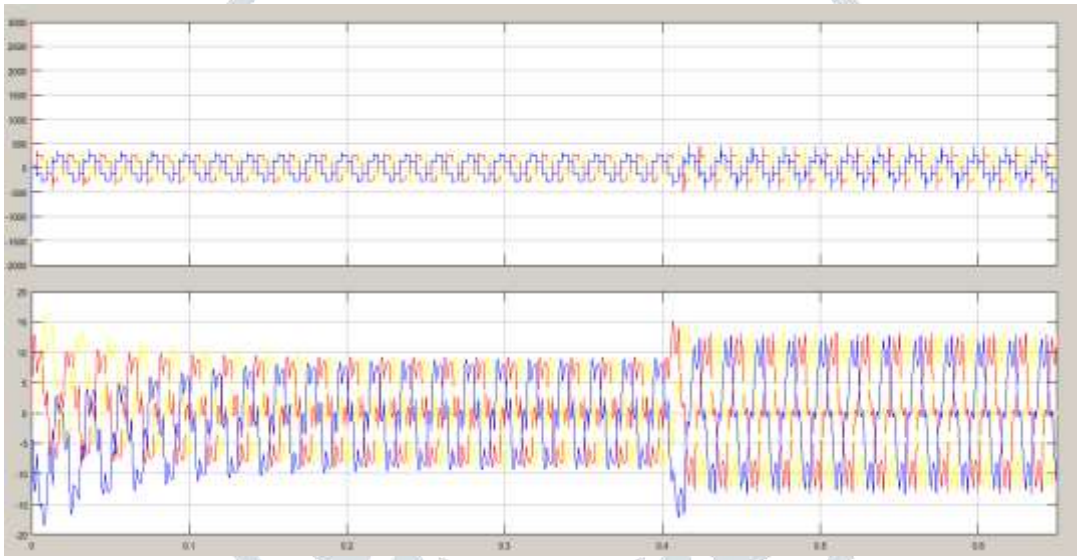

**Fig.21.** Three phase voltage and current measured at bus bar 2 during islanding occurs at 0.4 sec on DG-1 system

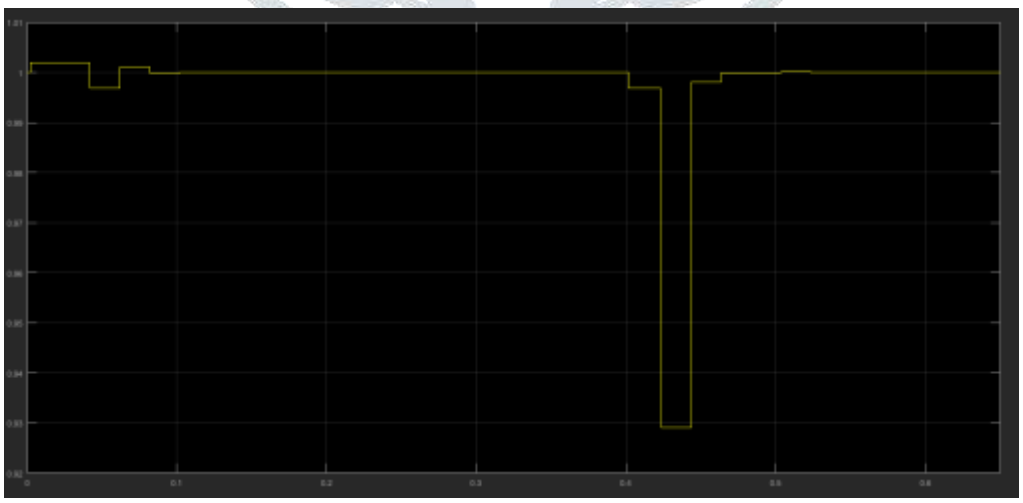

**Fig.22.** Frequency deviation response during case-2 DG-1 Islanding at 0.4 sec

Figure 20 shows three phase voltage and current measured at bus bar 1 i.e. AC output of solar PV array system-1 (40KW) during normal condition. Upper Y axis represent the three phase voltage in volts and lower Y axis shows the three phase current in Ampere. During case-2 DG-1 islanding condition, three phase voltage and current is disturb at 0.4 second due to single source acting from 0.4 to 1 second simulation time.

Figure 21 shows three phase voltage and current measured at bus bar 1 i.e. AC output of solar PV array system-1 (40KW) during normal condition. Upper Y axis represent the three phase voltage in volts and lower Y axis shows the three phase current in Ampere.

During case-2 DG-1 islanding condition, three phase voltage and current is disturb at 0.4 second due to single source acting from 0.4 to 1 second simulation time.

### 4.3 Case-3 Islanding at DG-2

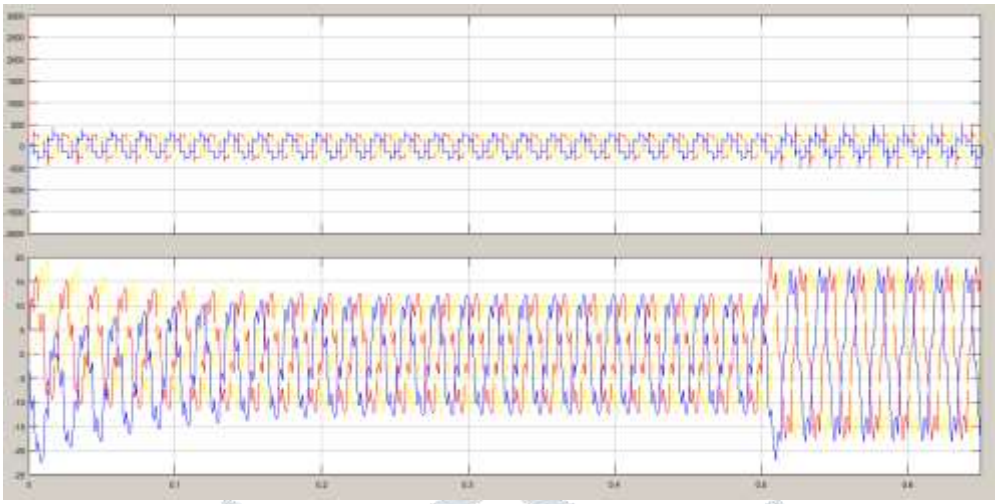

**Fig.23.** Three phase voltage and current measured at bus bar 1 during islanding occurs at 0.5 sec on DG-2 system

Figure 23 shows three phase voltage and current measured at bus bar 1 i.e. AC output of solar PV array system-1 (40KW) during case-2. Upper Y axis represent the three phase voltage in volts and lower Y axis shows the three phase current in Ampere. During case-3 DG-2 islanding condition, three phase voltage and current is disturb at 0.5 second due to single source acting from 0.5 to 1 second simulation time.

Figure 24 shows three phase voltage and current measured at bus bar 3 i.e. AC output after LC filter of solar PV array system-1 (40KW) during case-2. Upper Y axis represent the three phase voltage in volts and lower Y axis shows the three phase current in Ampere. During case-3 DG-2 islanding condition, three phase voltage and current is disturb at 0.5 second due to single source acting from 0.5 to 1 second simulation time.

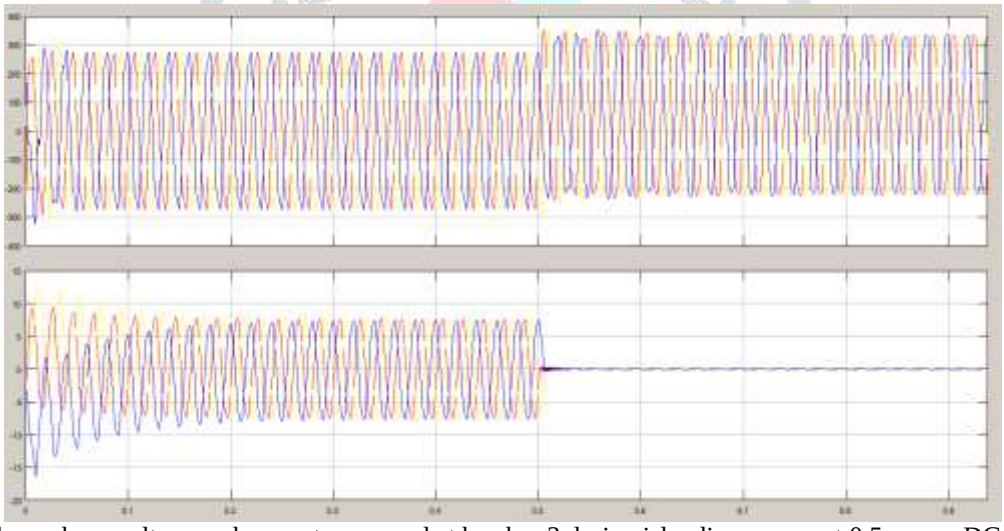

**Fig.24.** Three phase voltage and current measured at bus bar 3 during islanding occurs at 0.5 sec on DG-2 system

## V. CONCLUSION

The suggested technique is based on the wavelet transform as well as a novel classifier known as the Artificial Neural Network (ANN) and Adaptive Neuro Fuzzy Inference System (ANFIS). The suggested technique is tested on two DGs each with a 40 KW solar PV system linked to an AC Parallel RLC load at a point of common connection as per the rating in [1].

The system includes a photovoltaic (PV) unit as a DER that is connected to a voltage-sourced converter (VSC), an RL filter that connects the VSC to the PCC of a 0.4 kV LV network that feeds an RLC load, and a voltage-sourced converter (VSC) that connects the VSC to the PCC of a 0.4 kV LV network that feeds an RLC load. At the VSC input, the PV is represented as a continuous current source that delivers 300 V DC voltage. With a solar irradiance of 1000 kW/m2 and a panel temperature of 25 degrees Celsius, the PV unit is set to its maximum power point.

A 20 kW PV unit is termed DG in this case. It may, however, be readily substituted with any other RERs or ESSs. The integrated gate bipolar transistor's firing signals (IGBT).

Pulse width modulation (PWM) is used to create switches in the VSC. The PCC connects the DG to the DN, allowing it to function in either islanded or grid-connected mode. For the DN power source, the RLC impedance is internal.

We used the ANN and ANFIS classifiers to classify the islanding generator number in this study. It has been discovered that ANN classifies islanding events up to 100%, but ANFIS classifies generator islanding events up to 90%. As a consequence, it is evident that ANN provides the best classification results for detecting the number of islanding generators during an islanding event.

**REFERENCES**

[1] Gholami, M. "Islanding Detection Method of Distributed Generation Based on Wavenet." International Journal of Engineering 32.2 (2019): 242-248.
[2] Raza, Safdar, et al. "Minimum-features-based ANN-PSO approach for islanding detection in distribution system." *IET Renewable Power Generation* 10.9 (2016): 1255-1263.
[3] Shayeghi, Hossein, et al. "Optimal neuro-fuzzy based islanding detection method for Distributed Generation." *Neurocomputing* 177 (2016): 478-488.
[4] Vatani, Mehrnoosh, et al. "Relay logic for islanding detection in active distribution systems." *IET Generation, Transmission & Distribution* 9.12 (2015): 1254-1263.
[5] Wang, Yunqi, Jayashri Ravishankar, and Toan Phung. "Wavelet transform-based feature extraction for detection and classification of disturbances in an islanded micro-grid." *IET Generation, Transmission & Distribution* 13.11 (2018): 2077-2087.
[7] Khodaparastan, Mahdiyeh, et al. "A novel hybrid islanding detection method for inverter-based DGs using SFS and ROCOF." IEEE Transactions on Power Delivery 32.5 (2015): 2162-2170.
[8] Do, Hieu Thanh, et al. "Passive-islanding detection method using the wavelet packet transform in grid-connected photovoltaic systems." IEEE Transactions on power electronics 31.10 (2015): 6955-6967.
[9] Ghzaiel, Walid, et al. "Grid impedance estimation based hybrid islanding detection method for AC microgrids." Mathematics and Computers in Simulation 131 (2017): 142-156.
[10] Eshraghi, Alireza, and Reza Ghorbani. "Islanding detection and over voltage mitigation using controllable loads." Sustainable Energy, Grids and Networks 6 (2016): 125-135.
[11] Jia, Ke, et al. "An islanding detection method for multi-DG systems based on high-frequency impedance estimation." IEEE Transactions on sustainable energy 8.1 (2016): 74-83.
[12] Reddy, Ch Rami, and K. Harinadha Reddy. "Islanding detection using DQ transformation based PI approach in integrated distributed generation." International journal of control theory and applications 10.5 (2017): 679-690.
[13] Sun, Qinfei, et al. "An islanding detection method by using frequency positive feedback based on FLL for single-phase microgrid." IEEE Transactions on Smart Grid 8.4 (2015): 1821-1830.
[14] Chen, Xiaoyu, Jianyong Zheng, and Jun Mei. "Regional islanding detection method of large-scale grid-connected distributed photovoltaic power." 2017 International Conference on Electrical, Electronics and System Engineering (ICEESE). IEEE, 2017.